PROCEEDINGS OF SCIENCE

From Multiperipheral Models to BFKL Dynamics in Mueller–Navelet Jets

D. Vaccaro,[a,b,*] **G. Chachamis**[c,] **and A. Sabio Vera**[d,e]

[a] *Laboratório de Instrumentação e Física Experimental de Partículas, Av. Prof. Gama Pinto, 2, 1649-003, Lisbon, Portugal*

[b] *Departamento de Física, Instituto Superior Técnico, Universidade de Lisboa, Av. Rovisco Pais 1, 1049-001 Lisbon, Portugal*

[c] *Departamento de Ciencias, Universidad Pública de Navarra, Campus de Arrosadía, 31006 Pamplona, Spain*

[d] *Instituto de Física Teórica UAM/CSIC, Nicolás Cabrera 15, E-28049 Madrid, Spain*

[e] *Theoretical Physics Department, Universidad Autónoma de Madrid, E-28049 Madrid, Spain*

E-mail: dvaccaro@lip.pt, chachamis@gmail.com, a.sabio.vera@gmail.com

High-energy scattering often demands resumming large energy logarithms, beyond the reach of fixed-order QCD. Inspired by the old multiperipheral models, we study proton–proton collisions with a forward jet, a backward jet, and central mini-jets, using the BFKL framework. Jet rapidity distributions are used to search for BFKL effects, comparing PYTHIA8 predictions with those from the BFKLex Monte Carlo.

QCD at the Extremes (QCDEX2025)
1–5 Sept 2025
Online

*Speaker

PoS(QCDEX2025)044

1. Introduction

High-energy QCD provides a fertile ground for exploring the interplay between perturbative and non-perturbative regimes. At very large center-of-mass energies, scattering amplitudes are dominated by gluon exchange in the t-channel, where logarithms of the energy become large and require resummation. The Balitsky–Fadin–Kuraev–Lipatov (BFKL) [1] approach performs such a resummation, describing the exchange of a Reggeized gluon whose propagator acquires an energy-dependent dressing. A key challenge lies in identifying observables that are genuinely sensitive to BFKL dynamics [2] and not dominated by standard collinear evolution as described by the DGLAP equation [3]. Our strategy is to examine how multi-peripheral-type emissions [4] — an old concept from pre-QCD hadronic models — manifest within the modern BFKL framework, and how they can be probed through jet observables at the LHC.

In the multi-peripheral picture, high-energy collisions proceed through a chain of softly linked partonic clusters exchanging small momentum in the t-channel. Each produced particle is connected to the next through limited momentum transfer, leading to an approximately flat rapidity distribution. This behavior closely resembles the ladder structure emerging from the BFKL equation, where gluon emissions are strongly ordered in rapidity but not in transverse momentum. Revisiting classical multi-peripheral models (such as the Chew–Pignotti model) through the lens of BFKL dynamics may therefore shed light on the properties of the semi-hard regime of QCD.

We explore the connection between multi-peripheral emissions and Mueller–Navelet jet production [5]. This process, introduced several decades ago, consists of two high-p_T jets separated by a large rapidity interval, with additional emissions populating the gap. The extensive literature on Mueller–Navelet jets has mostly focused on observables such as azimuthal decorrelations and inclusive cross sections as probes of BFKL evolution. Here, we investigate a new class of observables that may provide complementary and more differential insight into the underlying dynamics. We present a preliminary Monte Carlo comparison between two event generators:

1. *BFKLex:* implements an iterative solution of the BFKL equation. For this study, we keep our precision at LLA [6].
2. *PYTHIA8:* includes hard scattering, parton shower, and multiple parton interactions (MPI) [7].

The comparison is performed at the parton level; in particular, hadronization is switched off in PYTHIA8 to ensure a consistent comparison, since BFKLex does not include hadronization effects.

2. Setup and Observables

We choose to analyze a set of esclusive observables, and to study the following process

$$p\, p \to j_1\, j_2\, X,$$

where X denotes the inclusive jet radiation. Jets are ordered in rapidity, and j_1 and j_2 are respectively the most backward and the most forward jet. We consider two different values of the center-of-mass energy, $\sqrt{s} = 8$ Tev and $\sqrt{s} = 13$ Tev. Final-state jets are reconstructed using the anti-kT algorithm

PoS(QCDEX2025)044

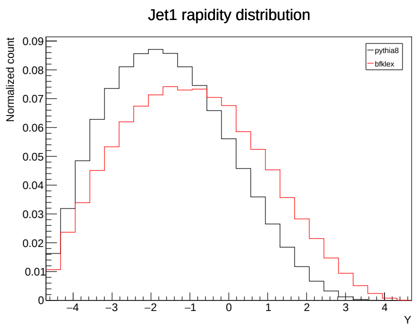

(a) Backward jet rapidity distribution.

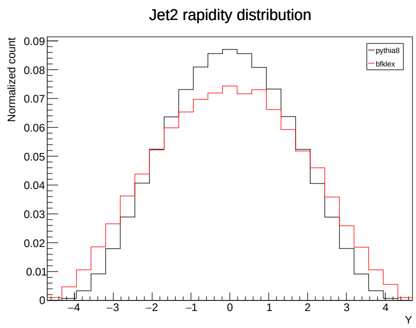

(b) Middle jet rapidity distribution.

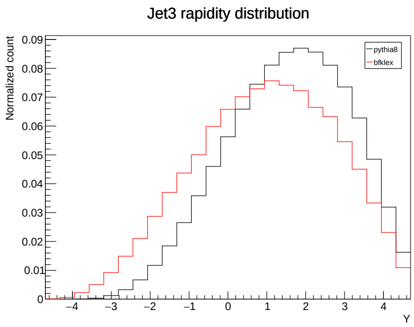

(c) Forward jet rapidity distribution.

Figure 1: BFKLex (red) vs. PYTHIA8 (black) comparisons of the rapidity distributions at 8 TeV for fixed multiplicity N =3.

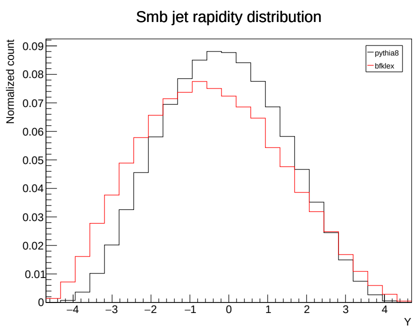

(a) Second most backward jet rapidity distribution.

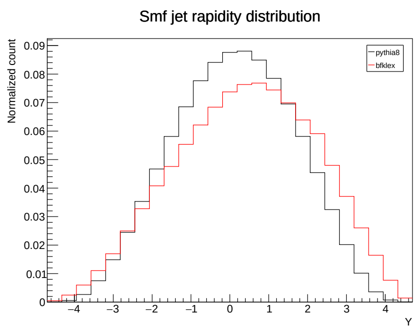

(b) Second most forward jet rapidity distribution.

Figure 2: BFKLex (red) vs. PYTHIA8 (black) comparisons at 8 TeV for the cumulative distribution of the second most backward and the second most forward jets arising from each event.

[9], with jet radius $R = 0.5$ and $R = 0.4$, corresponding respectively to 8 TeV and 13 TeV collisions. Each jet is required to have a transverse momentum greater than 20 Gev. Jets are selected to be inside the rapidity window (-4.7, 4.7). The following observables are analyzed:

1. *Fixed-multiplicity single-jet rapidity distribution*: For this observable, we select events with fixed jet multiplicity and plot the rapidity distributions for all ordered jets. For example, for

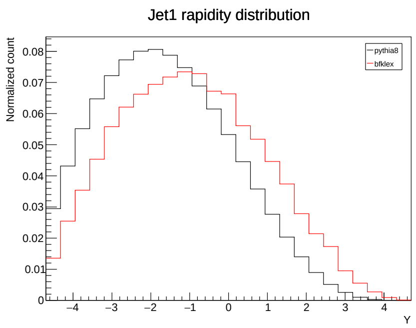

(a) Backward jet rapidity distribution.

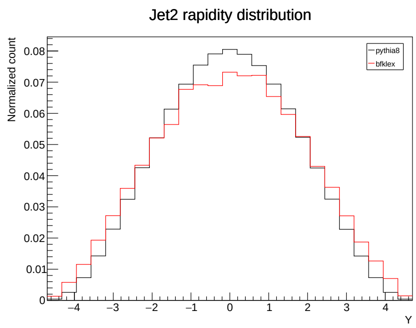

(b) Middle jet rapidity distribution.

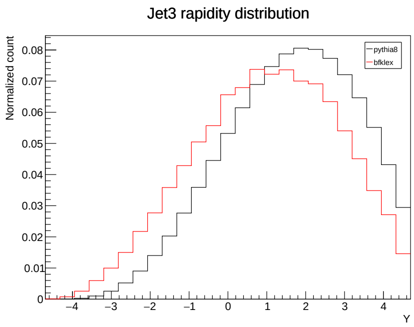

(c) Forward jet rapidity distribution.

Figure 3: BFKLex (red) vs. PYTHIA8 (black) comparisons of the rapidity distributions at 13 TeV for fixed multiplicity N =3.

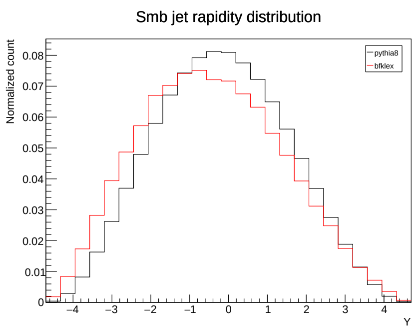

(a) Second most backward jet rapidity distribution.

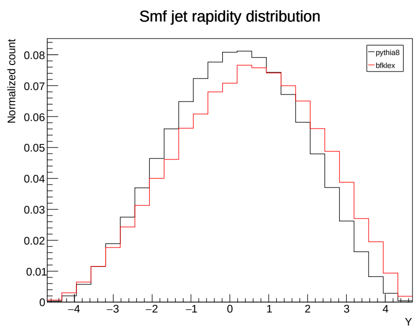

(b) Second most forward jet rapidity distribution.

Figure 4: BFKLex (red) vs. PYTHIA8 (black) comparisons at 13 TeV for the cumulative distribution of the second most backward and the second most forward jets arising from each event.

$N = 3$ events we will have three distributions, as in Fig. 1 for $\sqrt{s} = 8$ Tev, and Fig. 3 for $\sqrt{s} = 13$ Tev.

2. *Rapidity distribution of the second most forward/backward jets* (SMF/SMB): For this observable, we identify the second most backward and the second most forward jets in each event, regardless of the multiplicity of the event. The rapidity distributions of these two jets are then

collected from each event and shown separately in two distinct plots as in Fig. 2 and Fig. 4.

We observe that, in each plot, the BFKL curve (in red) is less peaked in the central region but exhibits broader tails compared to the PYTHIA8 curve (in black). This is a preliminary result, and it deserves further investigation, as it could potentially reflect differences in the underlying dynamics of the two generators. It is also worth noting that this behavior is more pronounced at 8 TeV, while at 13 TeV the difference is still present but appears less marked. Further studies, including jets rapidity–rapidity correlations and a comparison with HERWIG7 [8] Monte Carlo generator, will be conducted in the future.

3. Conclusions

In summary, we have explored multi-peripheral-type emissions within the BFKL framework through Mueller-Navelet jet observables. Preliminary comparisons between BFKLex and PYTHIA8 indicate distinct features in jet rapidity distributions, suggesting possible manifestations of BFKL dynamics. Future studies, including rapidity - rapidity correlations and comparisons with HERWIG7, will further clarify these effects and their phenomenological relevance.

Acknowledgements

We would like to thank Deniz Sunar Cerci and Salim Cerci for their insightful discussions and valuable suggestions. This work was partially supported by the Spanish Research Agency (Agencia Estatal de Investigación) through the grant IFT Centro de Excelencia Severo Ochoa SEV-2016-0597, and by the Spanish Government grant FPA2016-78220-P. It has also received funding from the European Union's Horizon 2020 research and innovation programme under grant agreement No. 824093. The work of G. Chachamis and D. Vaccaro was supported by the Fundação para a Ciência e a Tecnologia (Portugal) under project EXPL/FIS-PAR/1195/2021 (http://doi.org/10.54499/EXPL/FIS-PAR/1195/2021). G. Chachamis was also supported by the Fundação para a Ciência e a Tecnologia (Portugal) under project CERN/FIS-PAR/0032/2021 (http://doi.org/10.54499/CERN/FIS-PAR/0032/2021) and contract "Investigador FCT – Individual Call/03216/2017". D. Vaccaro was also supported by the Fundação para a Ciência e a Tecnologia (Portugal) under project PT-CERN PhD Grants - Call 2021/2.

References

[1] I. I. Balitsky and L. N. Lipatov, Sov. J. Nucl. Phys. 28 (1978) 822 [Yad. Fiz. 28 (1978) 1597]; E. A. Kuraev, L. N. Lipatov and V. S. Fadin, Sov. Phys. JETP 45 (1977) 199 [Zh. Eksp. Teor. Fiz. 72 (1977) 377]; E. A. Kuraev, L. N. Lipatov and V. S. Fadin, Sov. Phys. JETP 44 (1976) 443 [Zh. Eksp. Teor. Fiz. 71 (1976) 840].

[2] N. Bethencourt de León, G. Chachamis and A. Sabio Vera, Nucl. Phys. B 971 (2021) 115518; N. Bethencourt de León, G. Chachamis and A. Sabio Vera, Eur. Phys. J. C 81 (2021) 11, 1019; Baldenegro, C. and Chachamis, G. and Kampshoff, M. and Klasen, M. and Milhano, G. J. and Royon, C. and Sabio Vera, A., Phys. Rev. D 110 (2024) 11, 114027;

PoS(QCDEX2025)044

[3] V. N. Gribov, L. N. Lipatov, Sov. J. Nucl. Phys. 15, 438-450 (1972); V. N. Gribov, L. N. Lipatov, Sov. J. Nucl. Phys. 15, 675-684 (1972); L. N. Lipatov, Sov. J. Nucl. Phys. 20, 94-102 (1975); G. Altarelli, G. Parisi, Nucl. Phys. B 126, 298-318 (1977); Y. L. Dokshitzer, Sov. Phys. JETP 46, 641-653 (1977).

[4] G. F. Chew, A. Pignotti, Phys. Rev. 176, 2112-2119 (1968); C. E. DeTar, Phys. Rev. D 3, 128-144 (1971).

[5] A. H. Mueller, H. Navelet, Nucl. Phys. B 282, 727-744 (1987).

[6] G. Chachamis, A. Sabio Vera, PoS DIS 2013 (2013) 167; G. Chachamis, A. Sabio Vera, Phys. Lett. B 717 (2012) 458; G. Chachamis, A. Sabio Vera, Phys. Lett. B 709 (2012) 301; G. Chachamis, M. Deak, A. Sabio Vera, P. Stephens, Nucl. Phys. B 849 (2011) 28; F. Caporale, G. Chachamis, J. D. Madrigal, B. Murdaca, A. Sabio Vera, Phys. Lett. B 724 (2013) 127; G. Chachamis, A. Sabio Vera, C. Salas, Phys. Rev. D 87 (2013) 1, 016007; G. Chachamis, A. Sabio Vera, Phys. Rev. D 93 (2016) 7, 074004 ; G. Chachamis, A. Sabio Vera, JHEP 02 (2016) 064; G. Chachamis, A. Sabio Vera, Eur. Phys. J. C 78 (2018) 6, 496.

[7] Christian Bierlich et al., A comprehensive guide to the physics and usage of PYTHIA 8.3, arXiv:2203.11601.

[8] Bellm, J., Gieseke, S., Grellscheid, D. et al., Herwig 7.0/Herwig++ 3.0 release note, Eur. Phys. J. C 76, 196 (2016).

[9] M. Cacciari, G. P. Salam and G. Soyez, Eur. Phys. J. C 72, 1896 (2012) doi:10.1140/epjc/s10052- 012-1896-2 [arXiv:1111.6097 [hep-ph]].